Acta Biochim Biophys Sin 2012, 44: 490–502 | © The Author 2012. Published by ABBS Editorial Office in association with Oxford University Press on behalf of the Institute of Biochemistry and Cell Biology, Shanghai Institutes for Biological Sciences, Chinese Academy of Sciences. DOI: 10.1093/abbs/gms029.
Advance Access Publication 2 May 2012

Original Article

Angiogenesis inhibition and cell cycle arrest induced by treatment with Pseudolarix acid B alone or combined with 5-fluorouracil

Jingtao Liu, Wei Guo, Bo Xu, Fuxiang Ran, Mingming Chu, Hongzheng Fu, and Jingrong Cui*

State Key Laboratory of Natural and Biomimetic Drugs, School of Pharmaceutical Sciences, Peking University, Beijing 100191, China
*Correspondence address. Tel: +86-10-82802467; Fax: +86-10-82802467; E-mail: jrcui@bjmu.edu.cn

Angiogenesis inhibitors combined with chemotherapeutic drugs have significant efficacy in the treatment of a variety of cancers. Pseudolarix acid B (PAB) is a traditional pregnancy-terminating agent, which has previously been shown to reduce tumor growth and angiogenesis. In this study, we used the high content screening assay to examine the effects of PAB on human umbilical vein endothelial cells (HUVECs). Two hepatocarcinoma 22-transplanted mouse models were used to determine PAB efficacy in combination with 5-fluorouracil (5-Fu). Our results suggested that PAB (0.156–1.250 μM) inhibited HUVECs motility in a concentration-dependent manner without obvious cytotoxicity *in vitro*. *In vivo*, PAB (25 mg/kg/day) promoted the anti-tumor efficacy of 5-Fu (5 mg/kg/2 days) in combination therapy, resulting in significantly higher tumor inhibition rates, lower microvessel density values, and prolonged survival times. It was also demonstrated that PAB acted by blocking the cell cycle at both the G_1/S boundary and M phase, down-regulation of vascular endothelial growth factor, hypoxia-inducible factor 1α and cyclin E expression, and up-regulation of cdc2 expression. These observations provide the first evidence that PAB in combination with 5-Fu may be useful in cancer treatment.

Keywords combination therapy; angiogenesis inhibition; cell cycle arrest; Pseudolarix acid B; 5-fluorouracil

Received: November 15, 2011 Accepted: February 16, 2012

Introduction

Although chemotherapy is a mainstay of cancer treatment, it is also facing severe challenges in clinical practice [1]. Side effects and multi-drug resistance are two major problems of traditional treatment. Combination therapy has gained much attention in both experimental and clinical research [2]. Each drug in combination therapy could be used at its optimal dose without intolerant side effects. And another benefit of combination therapy is that it may reduce drug resistance, since one tumor is less likely to have resistance to multiple drugs simultaneously. Previous strategies mainly focused on using a combination of chemotherapeutics. Recently, researchers have found that using the first-line anti-cancer drug in combination with novel biological modalities for cancer treatment, such as angiogenesis inhibition, may provide compelling therapeutic regimens [1].

Angiogenesis refers to a process by which new capillaries sprout or split from the pre-existing vessels through the activation, proliferation, migration, and channelization of endothelial cells [3]. The growth of the vessels is required for tumor growth and metastasis, because the vessels provide nutrients to, and discharge waste from, tumor cells [4]. Since this theory was first proposed by Folkman in 1971, numerous angiogenesis inhibitors (AIs) have been explored for the discovery and development of novel anticancer drugs [4,5]. AIs are more frequently used in combination with chemotherapeutic drugs than as a monotherapy. In combined therapy, AIs can potentiate anti-tumor effects and reduce the dosage of cytotoxic agents required, possibly lowering the incidence of drug toxicity and tumor resistance [6]. Multi-targeted therapy is a basic principle of cancer therapy; therefore, agents displaying both anti-tumor and anti-angiogenic effects are particularly suitable for combined treatments. For this reason, combination therapy of Pseudolarix acid B (PAB) with other agents should be considered.

PAB is a traditional antifungal and pregnancy-terminating agent isolated from the Chinese medicinal plant *Pseudolarix kaempferi* [7]. Previous research has demonstrated that PAB exhibits considerable cytotoxicity toward several cancer cell lines, such as those of brain, colon, lung, breast, and renal origins [8]. Based on the studies of PAB-induced early pregnancy termination, scientists found that PAB might exhibit anti-angiogenic effects [9]. Recently, PAB has been reported to suppress

angiogenesis in human umbilical vein endothelial cells (HUVECs) proliferation, chick chorioallantoic membrane neovascularization, rat aorta sprout growth, and tube formation model by down-regulation of vascular endothelial growth factor (VEGF) and hypoxia-inducible factor 1α (HIF-1α) [7,10]. Further studies have also indicated that PAB arrests the cell cycle at the G_2/M [8,10] and regulates the expression of cell cycle-related proteins including cyclin B1 and cdc2 [11]. Nevertheless, there has been far less emphasis on combination therapy of PAB with chemotherapeutic drugs. In addition, little is known about the relationship between PAB toxicity and its efficacy. Furthermore, fewer studies on the effects of PAB are performed *in vivo* than *in vitro*. Therefore, in our experiments, we first utilized a high content screening (HCS) assay to examine whether PAB was cytotoxic and could suppress cell motility *in vitro*. After that, hepatocarcinoma 22 (H_{22})-transplanted mouse model was adopted to detect anti-tumor and anti-angiogenic effects of PAB in combination with the classic chemotherapeutic agent 5-fluorouracil (5-Fu). Finally, we explored the probable mechanisms of PAB combined with 5-Fu by utilizing flow cytometry (FCM) and western blot analyses.

Materials and Methods

Reagents

PAB ($C_{23}H_{28}O_8$, M: 432.464) was supplied by Professor Hongzheng Fu at Peking University (Beijing, China) as slight yellow powder. For *in vivo* experiments, PAB was dissolved in normal saline (NS; 0.9% NaCl) to the indicated concentration. For *in vitro* experiments, it was dissolved in phosphate-buffered saline (PBS). 5-Fu ($C_4H_3FN_2O_2$, M: 130.08) was purchased from Peking University Third Hospital as a fluorouracil injection (10 ml:0.25 g), and diluted in NS or PBS for experiments *in vivo* or *in vitro*, respectively. The primary antibodies anti-VEGF (rabbit), anti-HIF-1α (rabbit), anti-cyclin E (rabbit), anti-cdc2 (rabbit), anti-cdk2 (rabbit), anti-β-actin (mouse), and the horseradish peroxidase (HRP)-conjugated goat anti-rabbit and goat anti-mouse secondary antibodies were purchased from Santa Cruz (Santa Cruz, USA). Anti-cyclin B1 antibody was from Cell Signaling Technology (Beverly, USA).

Cell culture

HUVECs were isolated from human umbilical cord veins with a 0.1% type-I collagenase digestion at 37°C for 15 min as described previously [12]. The cells were maintained in medium 199 (M199, Gibco, New York, USA) supplemented with 10% fetal bovine serum (FBS, Gibco), 40 μg/ml endothelial cell growth supplement (Sigma, St Louis, USA), 100 U/ml penicillin and 100 μg/ml streptomycin at 37°C in a humidified atmosphere with 5% CO_2. Cells in passages 3–8 were used for the following experiments. Murine H_{22} ascites tumor cells were supplied by the cell bank of the pharmacology group of State Key Laboratory of Natural and Biomimetic Drugs, Peking University.

HCS cell motility assay

To determine the effects of PAB on endothelial cell movement, we used the HCS cell motility HitKit (Cellomics, Rockford, USA) as previously described [3,13]. After HUVECs were harvested and washed three times with serum-free culture medium, 50 μl of the cell suspension (1.0×10^4 cells/ml) was plated in each well of 96-well microplate (Corning, New York, USA). The microplates had been coated with rat-tail collagen (self-prepared, 2.5 mg/ml) and then covered with a lawn of microscopic fluorescent beads. The wells were randomly divided into the following groups (four wells repeat in each group): negative controls, 40 μl serum-free culture medium plus 10 μl PBS; positive controls, 40 μl culture medium with 10% FBS plus 10 μl PBS; and the experimental groups, 40 μl culture medium with 10% FBS and 10 μl PAB (at different concentrations of 0.156, 0.313, 0.625, 1.250, and 2.500 μM) or 5-Fu (5.000 μM) or PAB (1.250 μM) plus 5-Fu (5.000 μM). In this assay, FBS was used to stimulate cell migration. After a 24-h incubation, the cells were fixed with 5.5% formalin, permeabilized with permeabilization buffer, and stained with a rhodamine–phalloidin staining solution for the visualization of cytoskeleton and the beads according to the manufacturer's instructions. Finally, the microplates were read on a Cellomics ArrayScan HCS Reader (KineticScan HCS readers 2.2.0, Cellomics), which allows automated plate handling, focusing, cell image acquisition, analysis, and quantification by Cell Motility BioApplication software (Cellomics, Rockford, USA).

HCS cytotoxicity assay

We detected and quantified the change of HUVECs in the nuclear morphology and size, cell membrane permeability, and mitochondrial transmembrane potential induced by PAB and 5-Fu with the HCS multi-parameter cytotoxicity 2 kit (Cellomics). HUVECs were seeded in microplates (5×10^4 cells/ml, 90 μl/well) and incubated for 24 h. PAB (at different concentrations of 0.156, 0.313, 0.625, and 1.250 μM) or PAB (1.250 μM) plus 5-Fu (5.000 μM) were added to each well; negative and positive controls were exposed to PBS and 5-Fu (5.000 μM, 10 μl/well), respectively. After a 24-h incubation, the cells were treated with a permeability dye, stained with the mitochondrial membrane potential dye and Hoechst dye, and washed with 1× wash buffer according to the manufacturer's instructions. Finally, the wells were filled with 1× wash buffer

(200 μl/well) and evaluated on the ArrayScan HCS Reader. The cell images were captured and analyzed using an appropriate image-processing BioApplication software module.

Animals

Male ICR (Institute of Cancer Research) mice (specific pathogen-free, 4–6 weeks old, 18–22 g) were purchased from the Department of Laboratory Animal Science of Peking University Health Science Center (Beijing, China). All procedures for mouse care strictly followed the protocols approved by the Institutional Animal Care and Use Committee of Peking University.

Solid-type H_{22} mouse model

A transplanted solid-type H_{22} mouse model was established in syngeneic ICR mice to evaluate whether PAB would improve the anti-tumor effectiveness of 5-Fu *in vivo*. The ICR mice were implanted subcutaneously under the left arm with 3×10^6 cells/ml of murine H_{22} ascites tumor cells which were diluted with 0.9% NS solution and administered at a volume of 0.2 ml per mouse. Subsequently, the mice were randomly divided into the following four groups (nine mice in each group). Group 1: control group, mice were injected intraperitoneally (i.p.) every other day and intragingivally (i.g.) every day with NS, 0.1 ml/10 g body weight. Group 2: mice received an i.p. injection of 5-Fu (5 mg/kg body weight) every other day and a daily i.g. injection of NS as Group 1. Group 3: mice received an i.p. injection of NS as Group 1 and a daily i.g. injection of PAB (25 mg/kg body weight). Group 4: mice were injected with 5-Fu i.p. and PAB i.g. as described for Groups 2 and 3, respectively. Reagents treatment was initiated on Day 1 post-tumor implantation. Animal weights were measured on Days 1 and 11, and body weight gains were calculated. The dosages of PAB and 5-Fu were set at 25 mg/kg/day [8] and 5 mg/kg/2 days, respectively, as previously reported [6]. After being treated for 10 days, mice were sacrificed, and tumors were harvested, weighed, and captured. The inhibition on tumor growth and the change of body weight were calculated as follows: tumor growth inhibition rate (%) = [mean tumor weight of control group (g) − mean tumor weight of treatment group (g)]/mean tumor weight of control group (g) × 100%. The change of body weight (g) = mean body weight on Day 1 (g) − mean body weight on Day 11 (g) − mean tumor weight (g).

Ascitic fluid-type H_{22} mouse model

The efficacy of combination therapy was also examined in the ascitic fluid-type H_{22} mouse model. The H_{22} cell suspension (3×10^6 cells/ml, diluted with NS) was inoculated into 52 male ICR mice by i.p. injection. Mice were randomly divided into four groups, and the drug administration scheme was the same with that in solid-type model for 10 days. Body weight and general reaction were recorded every day. After drug treatment, three mice in each group were sacrificed, and tumor cells were harvested for cell cycle analysis. The survival rate of the other 10 mice in every group was calculated according to the following formula: prolonged survival time ratio = [mean survival time of experimental group (days) − mean survival time of control group (days)]/mean survival time of control group (days) × 100%.

Immunohistochemistry

Tumor samples were fixed in 10% formalin, embedded in paraffin, and sliced into 4-μm sections. Sections were subjected to hematoxylin and eosin (H&E) staining and immunostaining. For the latter, sections were deparaffinized in xylene and rehydrated. Endogenous peroxidase was blocked with 3% hydrogen peroxide for 10 min. The sections were boiled in 10 mM citrate buffer (pH 6.0) for 20 min as an antigen-retrieval procedure and then cooled to room temperature for 20 min. After being washed with Tris-buffered saline (TBS), all sections were incubated with an antibody specific for CD31 (Cluster of Differentiation 31/PECAM-1, 1 : 100, Santa Cruz) overnight. The sections were washed with TBS and treated with the Polymer HRP detection system (Polink-2 plus, goat anti rabbit, GBI, Mukilteo, USA) and 3,3′-diaminobenzidine tetrahydrochloride kit according to the manufacturer's instructions. Finally, all sections were slightly counterstained with hematoxylin, differentiated by chlorhydric acid alcohol, dehydrated, and mounted. The sections of immunohistochemistry and H&E staining were observed using an Olympus (Japan) BX 52 light microscope, and images were captured using an Olympus DP50 digital camera system. Endothelial cell clusters that were positive for CD31 and clearly separated from the adjacent tumor tissues were considered to be a single countable microvessel. The microvessel density (MVD) was quantified by the number of CD31-positive microvessels in ×200 microscope fields. Three images were collected from each section to evaluate the MVD.

Cell cycle analysis

Tumors from the mice implanted with fluid-type H_{22} cells were harvested, minced, and passed through a cell strainer to obtain single cell suspensions. The cells were washed with PBS and fixed with 70% ethanol overnight at −20°C. After centrifugation and washing, cells were treated with RNase (0.2 mg/ml), and stained with propidium iodide (PI, 0.1 g/ml). The cell cycle distribution was analyzed by FCM, and the percentages of stained nuclei (2N and 4N) by PI were calculated using CELLQuest Pro software (BD Pharmingen Biosciences, San Diego, USA).

Western blot analysis

The cells from solid tumor tissues and HUVECs were suspended in an appropriate volume of lysis buffer (1% Nonidet P-40, 10 mM Tris-HCl, 150 mM NaCl, 2 mM EDTA, and protease inhibitors including 2 mg/ml leupeptin, 2 mg/ml aprotinin, and 10 mg/ml phenylmethylsulfonyl fluoride, pH 7.4) and incubated on ice for 30 min with vortexing every 10 min. The cell lysates were cleared of cellular debris by centrifugation at 17,530 *g* at 4°C for 30 min. The Pierce protein assay (Pierce Biotechnology, Rockford, USA) was used to determine the supernatant protein concentrations. After denaturation by heating at 65°C for 10 min, equal amounts of protein (50 μg/10 μl) were separated on a 10% sodium dodecyl sulfate-polyacrylamide gel electrophoresis (SDS-PAGE) gel and transferred to nitrocellulose membranes (Hybond C; Amersham, Little Chalfont, UK) for 2 h. Membranes were blocked with 3% albumin fraction V [bovine serum albumin (BSA)] or 1% non-fat milk in TBS plus 0.05% Tween-20 (TBST). Membranes were incubated overnight at 4°C with primary antibodies against VEGF (1 : 1000), HIF-1α (1 : 500), cyclin B1 (1 : 2000), cyclin E (1 : 1000), cdc2 (1 : 1000), cdk2 (1 : 1000), and β-actin (1 : 2000), and diluted in 1.5% BSA in TBST. After being washed with TBST for 10 min three times, the membranes were incubated for 2 h with secondary antibodies (1 : 15,000). The membranes were washed four times in TBST for 15 min, and the immunoreactive bands were visualized using the ChemiDoc XRS system (Bio-Red, Hercules, USA) according to the manufacturer's instructions.

Reverse transcription-polymerase chain reaction

Reverse transcription-polymerase chain reaction (RT-PCR) was taken to semi-quantify the expression of *VEGF* mRNA and *HIF-1α* mRNA in drug-treated H22 tumor cells. Total RNA was extracted from frozen ascitic fluid samples using Trizol reagent (DingGuo, Beijing, China) according to the general protocol. A high-fidelity RT-PCR kit was used to prepare cDNA sample. About 1 μg total RNA was reverse-transcribed with a ReverTra Ace reverse transcriptase (DingGuo) in 20 μl reaction buffer. RT-PCR amplification was carried out for one cycle of 94°C for 5 min, followed by 30 cycles of 94°C for 30 s, 57°C for 30 s, and 72°C for 30 s, then one cycle of 72 °C for 5 min and held at 4°C. *β-Actin* was used as an internal control. The primer sequences were as follows: *VEGF*, 5′-ctggctatgctgttctca-3′ and 5′-aaataagggttccgatgc-3′; *HIF-1α*, 5′-gtgggagacgcctct aag-3′ and 5′-gcgacggctggacaactaca-3′; *β-Actin*, 5′-gta ttacggtatttcgtg-3′ and 5′-agagttacaagtggcaga-3′. The products were analyzed by gel electrophoresis on 1% agarose gels, stained with GoldView (DingGuo, Beijing, China) nucleic acid stain and visualized by the ChemiDoc XRS system.

Statistical analyses

Data were obtained from three independent experiments. All values were expressed as the mean ± standard deviation (SD). Statistical significance was determined by the Chi-square (χ^2) test (in the mice lifespan experiment) or the unpaired two-tailed Student's *t*-test (in all the other experiments). $P < 0.05$ was considered to be of statistical significance.

Results

PAB suppresses HUVECs motility

Endothelial cell migration is an important step in angiogenesis. The anti-angiogenic effect of PAB *in vitro* was characterized by the HCS cell motility assay on HUVECs. Serum-stimulated cells [**Fig. 1(A)**] migrated a greater distance than the negative controls, owing to serum stimulation. Compared with the positive controls, the tracks left by PAB-treated cells decreased in a concentration-dependent manner [**Fig. 1(A)**]. The statistical data in the bar graph indicated that PAB inhibited HUVECs motility in a dose-dependent manner [**Fig. 1(B)**], while 5-Fu contributed little to suppress cell movement.

PAB has less cytotoxicity than 5-Fu on HUVECs

To determine whether the PAB-induced cell motility reduction was due to cytotoxicity, we detected the markers of cell viability: the nuclear size, mitochondrial transmembrane potential, and cell membrane permeability by labeling HUVECs with fluorescent dyes. **Figure 2** indicates that there were no significant differences between the PBS controls and PAB groups except that the high-dosage group (PAB, 1.250 μM) exhibited a slight decline in the nuclear size and mitochondrial transmembrane potential. However, 5-Fu as a positive control showed a significant increase in cell permeability and a decrease in mitochondrial transmembrane potential. These results suggest that PAB exhibits much lower cytotoxicity than 5-Fu on endothelial cells under the anti-angiogenic concentration.

PAB inhibits solid-type H_{22} tumors growth in combination with 5-Fu

PAB (25 mg/kg/day) and 5-Fu (5 mg/kg/2 days) treatments were administered simultaneously, which had been determined previously [6,8]. As shown in **Table 1** and **Fig. 3**, the tumor weight and tumor size decreased substantially in the agent-treated group compared with in NS controls. The tumor inhibition rate was more than 60% in the combination group, whereas the inhibition rates were less than 40% in the single-agent groups. Significant differences in tumor weight were also observed between mice receiving single or combined treatments. The data showed that the body weight of every group increased during the treatment. The changes of

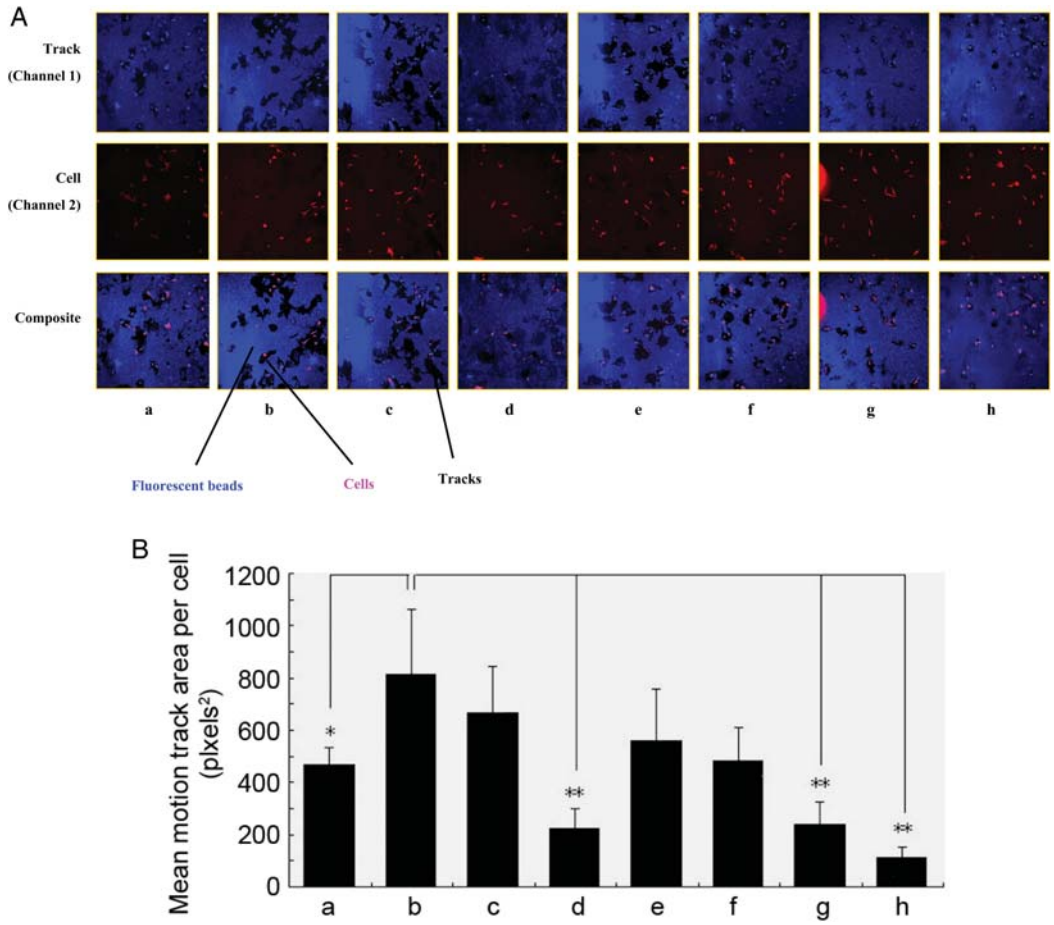

Figure 1 Effects of PAB and 5-Fu on HUVECs motility (A) The blue background indicated the fluorescent beads. Red or purple points were the cells either expressing rhodamine–phalloidin or having phagocytosed fluorescent beads. Black tails indicated cell movement, and these were noticeably reduced by PAB. (B) After the images were collected, the track area for each cell was measured by the Cell Motility BioApplication. According to manufacturer's instructions, the track area swept out by the cells is proportional to the integrated mean square displacement of cell movement. The output well feature 'Mean motion track area per cell' is representative of an average of the productive movement per cell within all selected tracks in one well. PAB significantly inhibited HUVECs movement at the concentration of 0.625 and 1.250 μM. $*P < 0.05$, $**P < 0.01$ vs. PBS+10% FBS group. a. PBS; b. PBS + 10% FBS; c. 5-Fu (5.000 μM) + 10% FBS; d. 5-Fu (5.000 μM) + PAB (0.625 μM) + 10% FBS; e. PAB (0.156 μM) + 10% FBS; f. PAB (0.313 μM) + 10% FBS; g. PAB (0.625 μM) + 10% FBS; h. PAB (1.250 μM) + 10% FBS.

body weight in the agent-treated groups were slightly higher than in the NS group; however, there were no statistically significant differences between any group (Table 1).

PAB prolongs the lifespan of mice with ascitic fluid-type H_{22} tumors in combination with 5-Fu

The ascitic fluid-type H_{22} mouse model was used to detect the effectiveness of PAB on the mouse lifespan in combination with 5-Fu. The results in **Fig. 4** show that the survival of mice in the treated groups was extended significantly compared with that in the control group. Moreover, the lifespan of mice in the combined therapy group was the longest among the four groups. All of the mice in the NS control group died between 12 and 19 days post-injection, whereas the mice in the combination group survived up to 40 days. The data in Table 2 illustrates that, in comparison with NS control, the prolonged survival time ratios of the 5-Fu and PAB groups were less than 20%, whereas the ratio reached nearly 80% in the combined treatment group.

Combination treatment of PAB and 5-Fu inhibits angiogenesis and induces necrosis in solid-type H_{22} tumors

To identify the *in vivo* effect of PAB on angiogenesis, each solid-type H_{22} tumor tissue was evaluated by MVD through immunohistochemical staining [14]. MVD is a prognostic biomarker of new-angiognetic process, using CD31/PECAM as a marker for vascular endothelium. In the images collected by a light microscope and a digital camera system, CD31-positive vessels were stained light yellow, whereas CD31-negative vessels were stained blue similar to adjacent cells (**Fig. 5**). Table 3 summarizes the MVD values for all four groups. A higher MVD value was detected in the NS control than in the single PAB and combination therapy groups; however, there were no

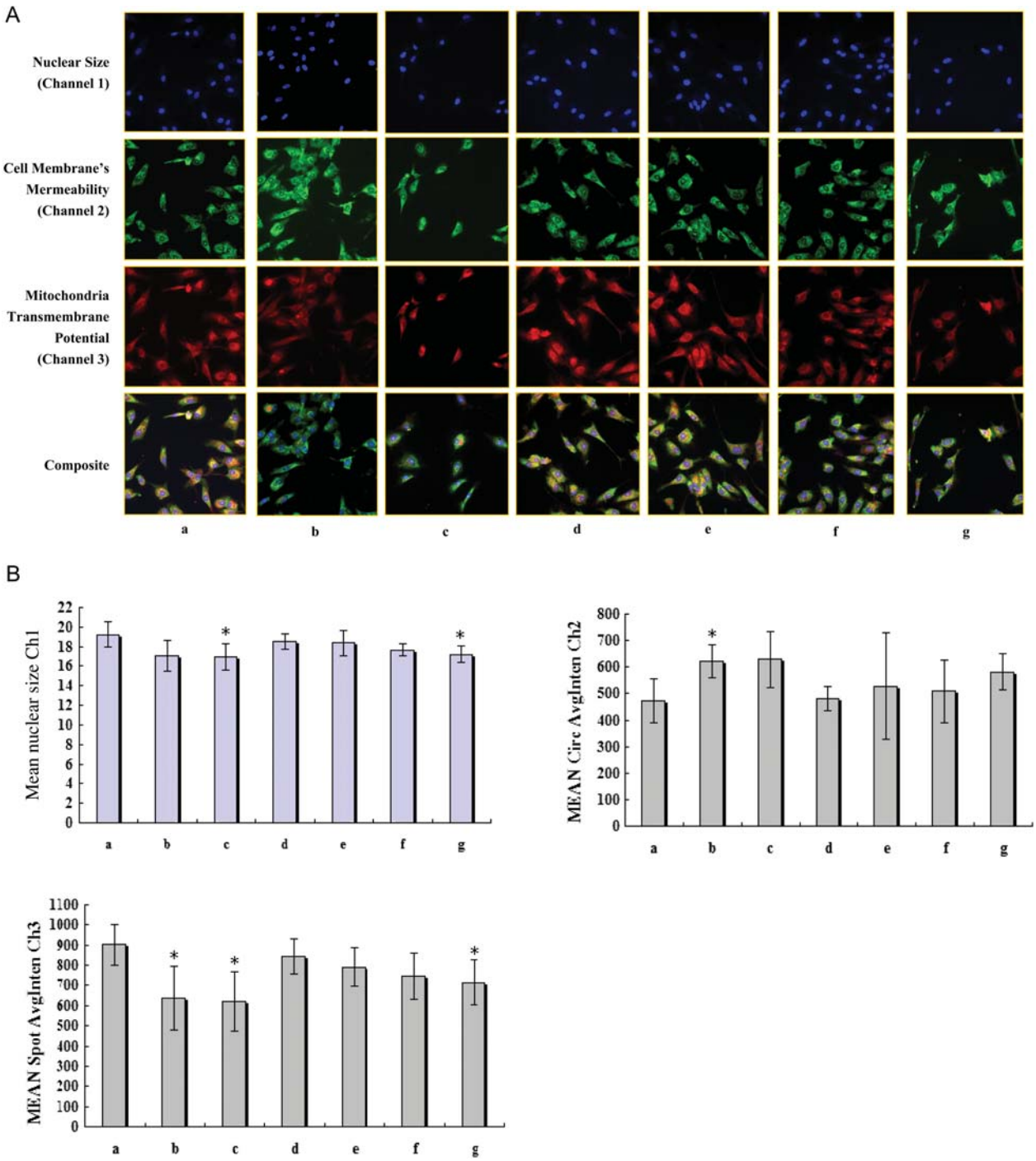

Figure 2 Cytotoxicity of PAB and 5-Fu on HUVECs (A) HUVECs were treated and stained with indicated dyes, and images were captured by the ArrayScan HCS Reader. The channels 1, 2, and 3 represents the Hoechst 33342 dye (blue), the permeability dye (green) and the mitochondrial membrane potential dye (red), respectively. (B) The quantification of the nuclear size, cell membrane's permeability and mitochondrial membrane potential. The data were calculated by the Cell Motility BioApplication software. *$P < 0.05$ vs. PBS control. a. PBS; b. 5-Fu (5.000 μM); c. 5-Fu (5.000 μM) + PAB (0.625 μM); e. PAB (0.156 μM); f. PAB (0.313 μM); g. PAB (0.625 μM); h. PAB (1.250 μM).

significant differences between the NS control and the 5-Fu group. Therefore, PAB substantially inhibited tumor neovascularization *in vivo*.

Pathological examinations of the tumor tissue were performed as shown in **Fig. 6**. In comparison with all other groups, the negative control was characterized by a compact arrangement of H_{22} cells with no apparent necrosis. The cells in the treated groups underwent obvious vacuolar degeneration of the cytoplasm and were in a dispersed arrangement. Coagulative necrosis and nuclear pyknosis of tumor cells around capillary vessels were observed, particularly in the 5-Fu and combination groups. The H_{22} tumor tissue

Table 1 Anti-tumor effects of PAB and 5-Fu treatments on the growth of H_{22}-transplanted tumors (mean ± SD, $n = 9$)

Treatment	Dose (mg/kg)	Body weight change (g)	Tumor weight (g)	The inhibition rate of tumor growth (%)
NS	0	6.2 ± 1.9	1.06 ± 0.29	–
5-Fu	5	6.9 ± 1.4	0.71 ± 0.27*	33.4
PAB	25	7.6 ± 1.9	0.69 ± 0.38**	35.4
5-Fu + PAB	5 + 25	7.0 ± 2.7	0.35 ± 0.11***$^{\triangle\triangle\#}$	60.6

The H_{22}-transplanted mice were treated with NS or agents for 10 days. NS (i.g. and i.p.), PAB (i.g.) and 5-Fu (i.p.) were administered simultaneously on Days 1, 3, 5, 7, and 9, whereas NS (i.g.) and PAB (i.g.) were administered as single treatments on Days 2, 4, 6, 8, and 10.

*$P < 0.05$, **$P < 0.01$, ***$P < 0.001$ vs. NS control. $^{\triangle\triangle}P < 0.01$ vs. 5-Fu group. $^{\#}P < 0.05$ vs. PAB group.

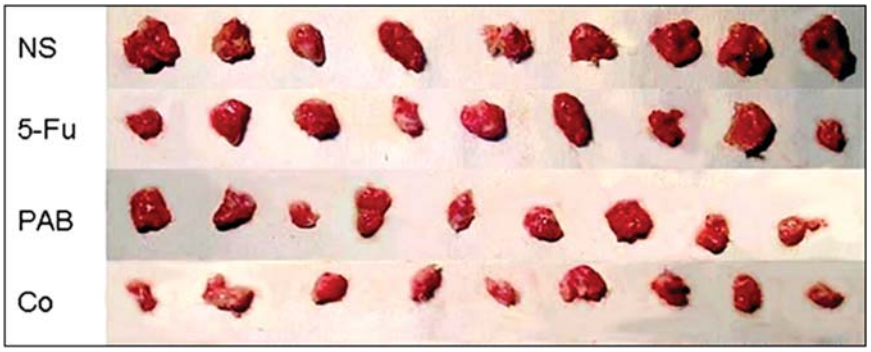

Figure 3 Anti-tumor effects of PAB and 5-Fu treatments on the growth of H_{22}-transplanted tumors ($n = 9$) The H_{22}-transplanted mice were treated with NS or agents for 10 days as described before. Tumor size in the combination therapy group was obviously less than that in the NS- and single-treated group.

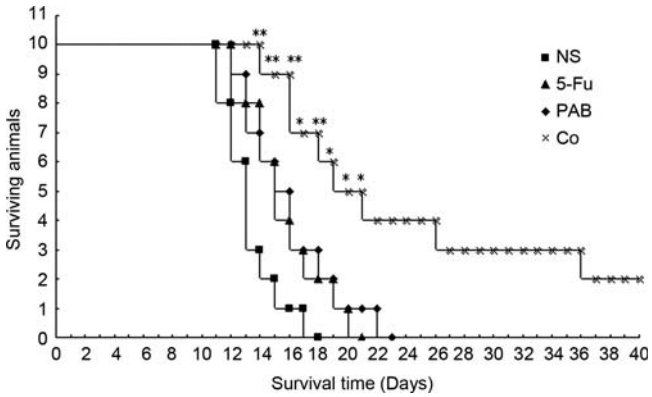

Figure 4 Effect of combined therapy on the lifespan of ascitic fluid-type H_{22}-transplanted mice ($n = 9$) All mice were treated with agents or NS for 10 days. The survival time of mice in agent-treated groups was prolonged compared with the NS control group. On the 40th day post-tumor implantation, the end of this experiment, two mice in the combined group were still alive. *$P < 0.05$, **$P < 0.01$ vs. NS control by the χ^2 test.

Table 2 Prolongation of survival of mice with ascitic fluid tumors by combination therapy (mean ± SD, $n = 9$)

Treatment	Dose (mg/kg)	Lifespan (days)	Prolonged survival time rate (%)
NS	–	14.1 ± 1.9	–
5-Fu	5	16.4 ± 2.7*	16.3
PAB	25	16.8 ± 3.1*	19.1
5-Fu + PAB	5+25	25.3 ± 9.8**$^{\triangle\#}$	79.4

*$P < 0.05$, **$P < 0.01$ vs. NS control. $^{\triangle}P < 0.05$ vs. 5-Fu group. $^{\#}P < 0.05$ vs. PAB group.

exhibited histopathological changes after treatment with PAB, 5-Fu, or the combination treatment.

PAB in combination with 5-Fu induces a double blockage of cell cycle in fluid-type H_{22} tumors

We then performed FCM to determine whether combination therapy could arrest the cell cycle in a fluid-type H_{22} transplanted model. The results showed that the percentage of cells in G_1 and G_2 phase increased in the 5-Fu- and PAB-treated groups, respectively. In combination therapy, the percentage of cells G_2/M phase and the ratio of cells in G_1 phase to in S phase (G_1/S) increased simultaneously (**Table 4** and **Fig. 7**). These results suggest that PAB and 5-Fu can suppress tumor growth and angiogenesis by arresting cell cycle progression.

PAB and 5-Fu alter protein expression in solid-type H_{22} tumors and HUVECs

Then, we investigated the possible mechanism of action of combination therapy using western blot analysis.

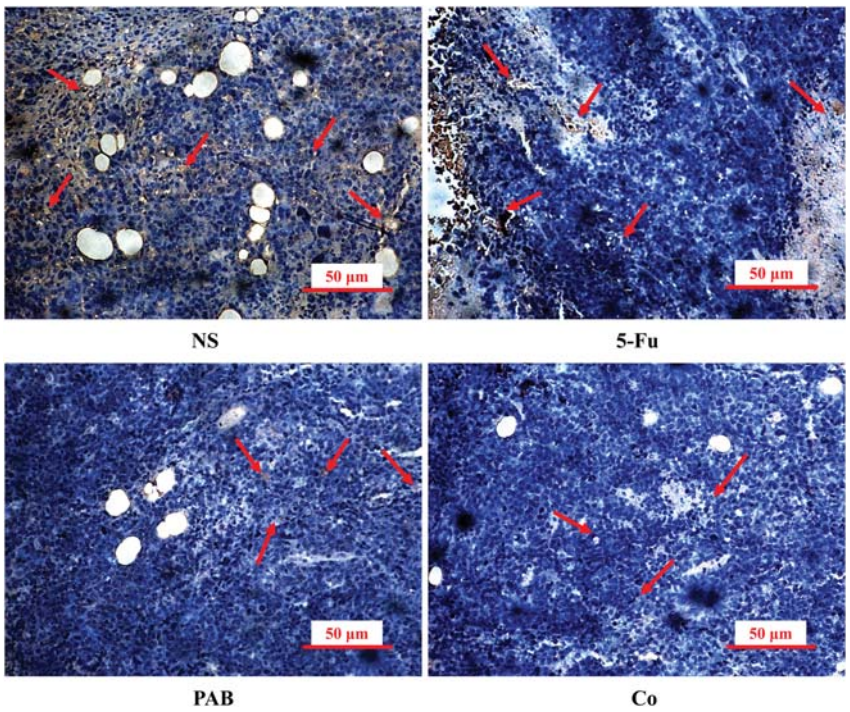

Figure 5 Immunostaining for microvessels with anti-CD31 in H_{22} tumor tissues The sections were treated as described previously, and the images were collected by an Olympus DP50 digital camera system. The cells were stained dark blue, and the CD31+ microvessels were bright yellow spots, as indicated with arrows. Bar, 12.5 μm.

Table 3 Values of MVD counts in H_{22} tumor tissues treated with PAB and 5-Fu (mean ± SD, $n = 3$)

Treatment	Dose (mg/kg)	MVD	Angiogenesis inhibition rate (%)
NS	0	71.3 ± 11.2	–
5-Fu	5	60.7 ± 13.1	19.0
PAB	25	41.3 ± 8.7*	42.1
5-Fu + PAB	5 + 25	32.0 ± 9.5**$^{\triangle}$	55.1

Data are summarized from 18 fields (three mice per group, two sections per mouse, and three fields per section).

*$P < 0.05$, **$P < 0.01$ vs. NS control. $^{\triangle}P < 0.05$ vs. 5-Fu group.

The proteins associated with angiogenesis were examined, including VEGF and its upstream regulator HIF-1α. As shown in **Fig. 8(A)**, compared with the NS control, VEGF and HIF-1α expression were substantially down-regulated in the PAB group and slightly decreased in the 5-Fu group, and further decreases were found in mice receiving the combined treatment. We also probed specific regulatory proteins of cell cycle, including cyclin B1, cdc2, cyclin E, and cdk2. The expression of cyclin B1 was similar in every group analyzed. It was slightly enhanced by PAB, but reduced by 5-Fu without statistical significance [**Fig. 8(B)**]. Compared with the NS group, the expression of cdc2 (p34) increased in the PAB and combined groups, whereas that of cyclin E declined in the 5-Fu and combination groups. No changes in cdk2 expression were detected. Similar results were also obtained *in vitro* as shown in **Fig. 9**, which could validate the *in vivo* data.

PAB and 5-Fu regulate mRNA expression of *VEGF* and *HIF-1α* in solid-type H_{22} tumors

Based on the above results, we further analyzed the mRNA expression of *VEGF* and *HIF-1α* in solid-type H_{22} tumors to investigate whether the combination therapy could induce protein expression changes. RT-PCR results revealed that the expression of both *VEGF* and *HIF-1α* mRNA decreased in the single-agent group (especially in the PAB-treated group) compared with that in the negative control, and further reduction was observed in the combination group (**Fig. 10**).

Discussion

Combination therapy plays an essential role in the clinical treatment of malignant tumors, and the simultaneous administration of AIs and chemotherapy agents has become a promising strategy [1]. Targeting tumor blood vessel growth can suppress neoangiogenesis and temporarily normalize tumor vessel structure, which may enhance tumor sensitivity to chemotherapy [15,16]. Therefore, it is possible that AIs not only potentiate the anticancer activity but also decrease the dosage of cytotoxic agent needed.

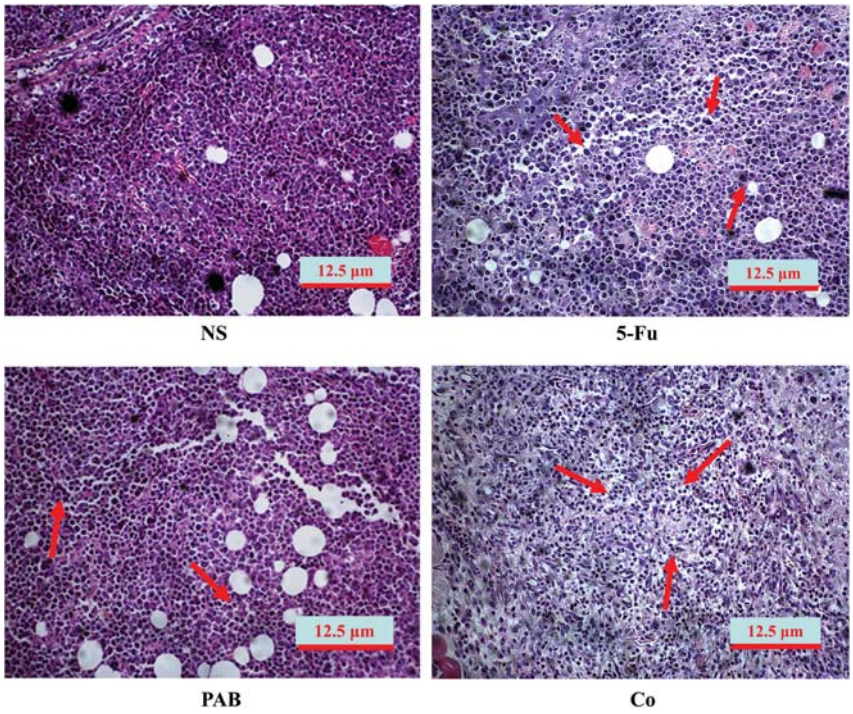

Figure 6 Photomicrographs of H_{22} tumor samples treated with PAB and 5-Fu The H&E-stained sections were observed and photographed using an Olympus light microscope (BX 52) and digital camera system (DP50). H_{22} tumor cells were arranged compactly in the NS control samples, whereas coagulative necrosis and nuclear pyknosis occurred in every agent-treated group (as indicated by arrows), particularly in the 5-Fu and combination groups. Bar, 12.5 μm.

Table 4 Quantitative analysis of the cell cycle distribution of H_{22} fluid-type tumors treated with PAB and 5-Fu (mean ± SD, $n = 3$)

Treatment	Dose (mg/kg)	G_1 (%)	S (%)	G_2+ M (%)	Ratio of G_1/S
NS	0	18.63 ± 3.94	44.00 ± 4.76	37.37 ± 2.89	0.430 ± 0.117
5-Fu	5	57.07 ± 2.07***	33.86 ± 2.80*	12.07 ± 4.86$^{**\#\#}$	1.601 ± 0.071$^{***\#\#\#}$
PAB	25	16.14 ± 3.49	34.14 ± 4.51	49.71 ± 7.35$^{\triangle\triangle}$	0.472 ± 0.081$^{\triangle\triangle\triangle}$
5-Fu + PAB	5 + 25	21.32 ± 2.26$^{\triangle\triangle\triangle}$	23.96 ± 4.46$^{**\triangle\#}$	54.72 ± 2.34$^{**\triangle\triangle\triangle}$	0.922 ± 0.269$^{*\triangle\#}$

$^{*}P < 0.05$, $^{**}P < 0.01$, $^{***}P < 0.001$ vs. NS control. $^{\triangle}P < 0.05$, $^{\triangle\triangle}P < 0.01$, $^{\triangle\triangle\triangle}P < 0.001$ vs.5-Fu group. $^{\#}P < 0.05$, $^{\#\#}P < 0.01$, $^{\#\#\#}P < 0.001$ vs. PAB group.

PAB is a natural diterpenoid compound that possesses both cytotoxic and anti-angiogenic activities [8,10,11]. This dual action enables PAB to exhibit anti-tumor effects via several distinct mechanisms; however, it is also difficult to distinguish these mechanisms. For this reason, we first examined the effects of PAB on HUVECs using the HCS assay. We chose this assay rather than a conventional angiogenesis model because it can differentiate between anti-angiogenic and cytotoxic activity. Endothelial cell movement is a critical step during tumor-induced angiogenesis [10], which is the foundation of neovascularization and tumor metastasis. In our work, the HCS cell motility assay showed that PAB significantly suppressed HUVECs migration and eliminated the effect of cell number on cell motility. In the HCS cytotoxicity assay, PAB exhibited much less toxicity than 5-Fu on HUVECs by measuring the nuclear size, membrane permeability status, and mitochondrial transmembrane potential. These results suggested that PAB might inhibit cell migration at lower concentrations than induced cytotoxicity. It may be concluded that the anti-angiogenic activity of PAB was due to its direct suppression of endothelial cell motility, instead of cellular toxicity [3,13].

After confirming that moderate doses of PAB could inhibit angiogenesis with a little toxicity *in vitro*, we further assessed the effectiveness of combination therapy with PAB and chemotherapy agents. The H_{22} transplant model was used because we are interested in anti-cancer effects on hepatocellular carcinoma (HCC) cells. Multi-drug resistance gene (*MDR1*) and P-glycoprotein (P-gp) expressions are enhanced in HCC compared with in normal liver cells, which may result in a poor response to chemotherapy in clinical trials [17]. Previous studies have

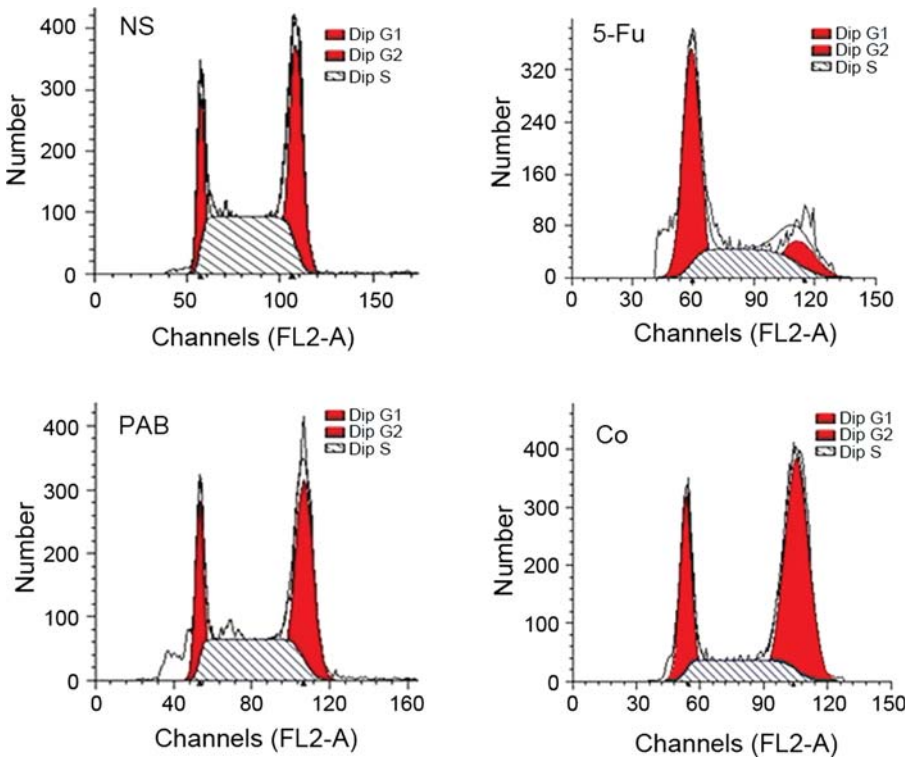

Figure 7 Effect of PAB combined with 5-Fu on the H22 fluid-type tumor cell cycle progression ($n = 3$) In each group, H_{22} fluid-type tumor cells were collected from three mice after treatment. Cell cycle distribution was analyzed by FCM.

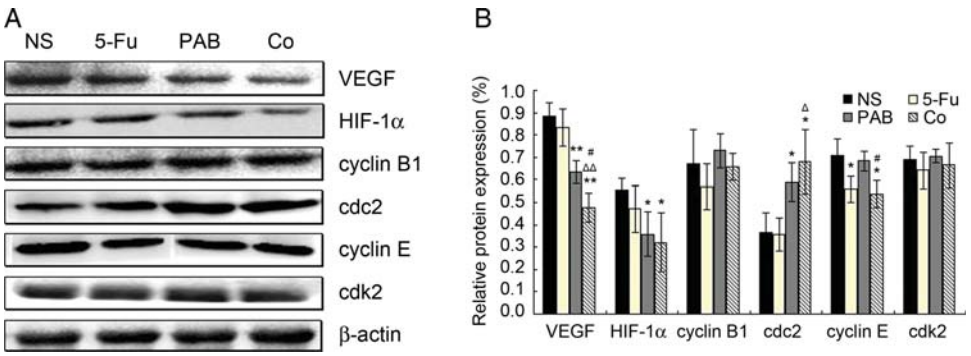

Figure 8 Effects of 5-Fu and PAB on the expression of related proteins in solid-type H_{22} tumor tissues ($n = 3$) (A) Western blot was used to detect related protein expression in ICR mice. (B) Quantification of the related protein expression from three mice per group. β-Actin was examined as a loading control. $^{*}P < 0.05$, $^{**}P < 0.01$ vs. NS control. $^{\triangle}P < 0.05$, $^{\triangle\triangle}P < 0.01$ vs.5-Fu group. $^{\#}P < 0.05$ vs. PAB group.

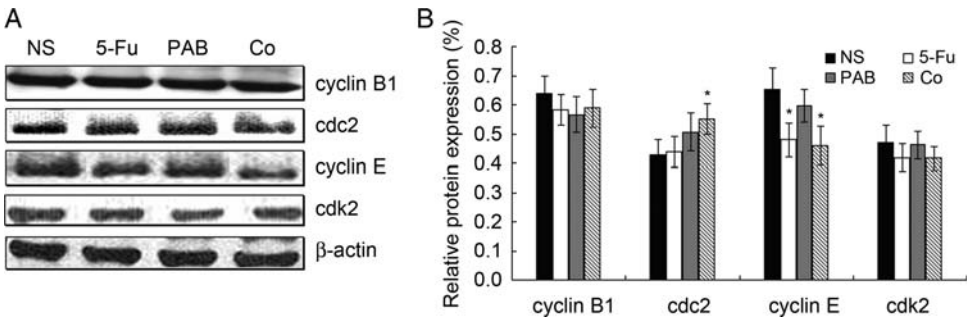

Figure 9 Effects of 5-Fu and PAB on the expression of cyclins and cdks in HUVECs ($n = 3$) (A) Whole cell extracts were prepared and analyzed by western blot. (B) Quantification of the related protein expression from three mice per group. β-Actin was examined as a loading control. $^{*}P < 0.05$ vs. NS control.

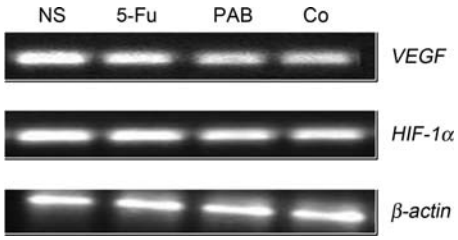

Figure 10 Effects of 5-Fu and PAB on the mRNA expression of *VEGF* and *HIF-1α* in solid-type H_{22} tumor tissues ($n = 3$) After treatment for 9 days, H_{22} tumors from three mice per group were harvested and RT-PCR analysis was used to detect *VEGF* and *HIF-1α* mRNA level. β-*Actin* was examined as a loading control.

suggested that 5-Fu is remarkably effective for the treatment of advanced HCC, especially in combination therapy [18]. Therefore, in this study, H_{22}-transplanted mice were treated with PAB combined with 5-Fu. Our strategy successfully reduced the dosage of 5-Fu with a non-toxic concentration of PAB and induced a stronger anti-tumor effect than single-agent treatment [6,8]. Compared with the single-agent groups, the tumor inhibition rate increased almost 30% when combination therapy was used. Differences between the monotherapy group and the combination group were significant. In the ascitic fluid-type H_{22} mouse model, the survival time of mice in the combination group was prolonged significantly in comparison with mice receiving NS. Although the therapeutic efficacy was enhanced with the combination of PAB and 5-Fu, no side effects on body weight were observed. In comparison with the NS and 5-Fu groups, the body weight gain was slightly higher after the combined treatment. H&E staining revealed that there were many histopathological changes in the agent-treated groups, such as tumor cell necrosis, vacuolar degeneration, dispersed arrangement, and nuclear pyknosis. These abnormal cells were observed more frequently in the tumor tissues treated with 5-Fu or combination therapy. MVD is an important indicator for measuring tumor angiogenesis; it is often assessed by determining the expression levels of CD31 using immunohistochemical staining [14]. The results from our studies indicated that the values of MVD in the PAB and combination groups were approximately half of those in the NS control group. Although a slight decline in MVD in the 5-Fu group was observed in comparison with NS control, the difference was not statistically significant. Taken together, the above data suggested that PAB promoted the anti-tumor effects of low-dose 5-Fu by suppressing tumor angiogenesis.

Based on the above results, we explored the mechanism of action of the combination therapy in ICR mice using FCM analysis and western blot analysis. Cell cycle arrest suppresses cell proliferation and may induce apoptosis. Both cytotoxic agents and AI can alter the cell cycle distribution. Previous researches have found that PAB could dramatically arrest the cell cycle at the G_2/M phase without G_2 checkpoint activation [8,10]. Subsequent studies have revealed that PAB-treated cells were arrested at M phase rather than at the G_2/M transition [19]. PAB has been shown to disassemble cellular microtubule networks and to disrupt the formation of mitotic spindles [8,19]. The chemotherapy agent 5-Fu, unlike PAB, is a pyrimidine anti-metabolite cytotoxin. It blocks DNA synthesis by inhibiting thymidylate synthetase and RNA incorporation during the S phase of the cell cycle [20]. Many experiments have demonstrated that there is a relationship between the anticancer efficacy of 5-Fu and the arrest of the cell cycle at the G_1/S phase [18,20]. Until now, there has been no evidence whether the enhancement of PAB combined with 5-Fu was related to cell cycle arrest. Our FCM results suggested that compared with the NS control, treatment with PAB or 5-Fu individually induced a cell cycle arrest at the G_2/M or the G_1 phase, respectively. Although the percentage of cells in the G_1 phase was almost alike in the NS control and the combination group, the ratio of cells in the G_1 phase to that in the S phase (G_1/S) increased significantly when mice were treated with two agents. Thus, the combination therapy led to cell cycle arrest at both the G_1/S and G_2/M phases. The synergistic effect of PAB in combination with 5-Fu can be illustrated by the double blockage of cell cycle.

Western blot analysis indicated that combination therapy down-regulated the expression of VEGF, HIF-1α, and cyclin E, whereas the cdc 2 expression level was up-regulated. VEGF is an essential activator involved in the pathologic link between angiogenesis and tumor growth [21]. As a highly specific endothelial cell mitogen, VEGF can promote endothelial cell proliferation, migration, and survival, resulting in tumor blood vessel formation [22]. It has been reported that VEGF expression may be enhanced by hypoxia, which is under the control of the transcription factor HIF-1α [23]. In many human cancers, HIF-1α levels were closely associated with increased vascularity and tumor progression [7]. Therefore, both VEGF and HIF-1α have been attractive targets for anti-cancer treatment. Previous research has shown that through accelerating HIF-1α protein degradation, PAB could abrogate the paracrine stimulation of VEGF and KDR/flk-1 phosphorylation, followed by down-regulation of the PI_3K/Akt and MAPK/ERK signaling pathways [11]. In our experiments, we found that the levels of mRNA and protein expression of HIF-1α and VEGF were concordant with CD31 staining results. PAB inhibited angiogenesis through the down-regulation of *VEGF* gene at the transcription and translation levels, which caused a reduction of CD31 expression in blood vessels. It is worthwhile to note that the suppression of protein expression was more obvious in the

mice receiving combination treatment. This may be because the cytotoxicity of 5-Fu resulted in the impairment of normal physiological function in tumor tissues, leading to a slight decline in VEGF and CD31 levels. These results further supported the idea that the angiogenic inhibition contributed to potentiate the anti-cancer activity. The cyclin is an important protein family that mediates the cell cycle via binding to a highly conserved family of protein kinases, the cdks. As an activator of progression from G_2 to M phase, the cyclin B and cdc2 genes are transcribed, and these mRNAs are stabilized from the end of the S phase [24]. During early mitosis, cyclin B1 relocates from the cytosol to the nucleus, and the degradation of cyclin B1 begins at the late phase of mitosis [19]. Our results indicated that the expression of cyclin B1 was reduced in the 5-Fu group and slightly increased in the PAB group, whereas its level in the combined therapy group was equivalent to that of the NS control group. Owing to the PAB-induced arrest of the cell cycle at M phase [19], cyclin B1 expression in PAB-treated tumor cells was up-regulated. Although 5-Fu is mainly involved in the G_1/S arrest, there is a relationship between 5-Fu and cyclin B1. On the one hand, 5-Fu can increase the expression of p53 in H_{22} tumor cells, which may negatively regulate cyclin B1 transcription [6,20]. On the other hand, the arrest of the cell cycle at the G_1/S transition by 5-Fu is likely to halt the initiation of cyclin B1 transcription in S phase. Both positive and negative regulations occur in the combination treatment, thus no changes in cyclin B1 expression were found compared with the NS group. Cdc2 expression levels were elevated in the PAB group, indicating that PAB induced a mitotic arrest [24]. G_1 progression and G_1/S transition are regulated by the assembly of cdk2 with cyclin E [6]. In the 5-Fu group, the expression of cyclin E was down-regulated, which is associated with a G_1/S arrest. Combination therapy both up-regulated cdc2 and down-regulated cyclin E expression, leading to the double blockage of the cell cycle as observed by FCM.

In summary, PAB could display an anti-motility function *in vitro* and improve the anti-cancer effects of 5-Fu in H_{22}-transplanted mouse models through angiogenesis inhibition and cell cycle arrest. The lifespan of mice was prolonged when treated with combined therapy. The mechanism of action of PAB was mainly associated with VEGF, HIF-1a, cyclins, and cdc protein expression. Further research is needed to clarify whether there is a relationship between the HIF-1α/VEGF signaling pathway and the cyclin B1/cdc2 heterodimer in the combination therapy. However, in view of improving agent solubility, the structural modification of PAB should be considered. These observations provide the first evidence that PAB, in combination with 5-Fu, may be useful for treating cancer.

Funding

This research is supported by grants from the 11th Five Years Key Program—the Comprehensive Center for Drug Discovery and Development, Peking University (2009ZX09301−010).

References

1 Bschof M, Abdollahi A, Gong P, Stoffegen C, Lipson KE, Debus JU and Weber KJ, *et al*. Triple combination of irradiation, chemotherapy (pemetrexed), and VEGF inhibition (SU5416) in human endothelial and tumor cells. Int J Radiat Oncol Biol Phys 2004, 60: 1220−1232.
2 Harari PM and Huang SM. Head and neck cancer as a clinical model for molecular targeting of therapy: combining EGFR blockade with radiation. Int J Radiat Oncol Biol Phys 2001, 49: 427−433.
3 Liu JT, Xu B, Li M, Zhou Y and Cui JR. Inhibition of angiogenesis by DADAG *in vivo* and *in vitro*. J Chin Pharmaceut Sci 2010, 19: 177−185.
4 Bisacchi D, Benelli R, Vanzetto C, Ferrari N, Tosetti F and Albini A. Anti-angiogenesis and angioprevention: mechanisms, problems and perspectives. Cancer Detect Prev 2003, 27: 229−238.
5 Folkman J. Tumor angiogenesis: therapeutic implications. N Engl J Med 1971, 285: 1182−1186.
6 Jia L, Xu B, Guo W, Ge ZM, Li RT and Cui JR. Enhanced antitumor effect and mechanism of TM208 in combination with 5-fluorouracil in H_{22} transplanted mice. J Chin Pharmaceut Sci 2011, 20: 615−626.
7 Li MH, Miao ZH, Tan WF, Yue JM, Zhang C, Lin LP and Zhang XW, *et al*. Pseudolaric acid B inhibits angiogenesis and reduces hypoxia-inducible factor 1alpha by promoting proteasome-mediated degradation. Clin Cancer Res 2004, 10: 8266−8274.
8 Wong VK, Chiu P, Chung SS, Chow LM, Zhao YZ, Yang BB and Ko BC. Pseudolaric acid B, a novel microtubule-destabilizing agent that circumvents multidrug resistance phenotype and exhibits antitumor activity *in vivo*. Clin Cancer Res 2005, 11: 6002−6011.
9 Wang WC and Gu ZP. Efects of pseudolaric acld B on blood flows of endometrium and myometrium in pregnant rats. Acta Pharmacol Sin 1991, 12: 423−425.
10 Tong YG, Zhang XW, Geng MY, Yue JM, Xin XL, Tian F and Shen X, *et al*. Pseudolarix acid B, a new tubulin-binding agent, inhibits angiogenesis by interacting with a novel binding site on tubulin. Mol Pharmacol 2006, 69: 1226−1233.
11 Tan WF, Zhang XW, Li MH, Yue JM, Chen Y, Lin LP and Ding J. Pseudolarix acid B inhibits angiogenesis by antagonizing the vascular endothelial growth factor-mediated anti-apoptotic effect. Eur J Pharmacol 2004, 499: 219−228.
12 Jaffe EA, Nachman RL, Becker CG and Minick CR. Culture of human endothelial cells derived from umbilical veins. Identification by morphologic and immunologic criteria. J Clin Invest 1973, 52: 2745−2756.
13 Wang XH, Xu B, Liu JT and Cui JR. Effect of β-escin sodium on endothelial cells proliferation, migration and apoptosis. Vasc Pharmacol 2008, 49: 158−165.
14 Kumar I, Staton CA, Cross SS, Reed MW and Brown NJ. Angiogenesis, vascular endothelial growth factor and its receptors in human surgical wounds. Br J Surg 2009, 96: 1484−1491.

15 Ryan CJ, Lin AM and Small EJ. Angiogenesis inhibition plus chemotherapy for metastatic hormone refractory prostate cancer: history and rationale. Urol Oncol 2006, 24: 250–253.
16 Bocci G, Falcone A, Fioravanti A, Orlandi P, Di Paolo A, Fanelli G and Viacava P. Antiangiogenic and anticolorectal cancer effects of metronomic irinotecan chemotherapy alone and in combination with semaxinib. Br J Cancer 2008, 98: 1619–1629.
17 Huang CC, Wu MC, Xu GW, Li DZ, Cheng H, Tu ZX and Jiang HQ, *et al*. Overexpression of the MDR1 gene and P-glycoprotein in human hepatocellular carcinoma. J Natl Cancer Inst 1992, 84: 262–264.
18 Yin H, Xie F, Zhang J, Yang Y, Deng B, Sun J and Wang Q. Combination of interferon-α and 5-fluorouracil induces apoptosis through mitochondrial pathway in hepatocellular carcinoma in vitro. Cancer Lett 2011, 306: 34–42.
19 Duan SW, Xu B, Chen YL, LI M, Fu HZ and Cui JR. Explore the mechanism of inhibitory effects of Pseudolaric acid B on MCF-7 cells by high content analysis. Prog Biochem Biophys 2010, 37: 1313–1322.
20 Tseng YS, Tzeng CC, Chiu AW, Lin CH, Won SJ, Wu IC and Liu HS. Ha-ras overexpression mediated cell apoptosis in the presence of 5-fluorouracil. Exp Cell Res 2003, 288: 403–414.
21 Alshenawy HA. Prognostic significance of vascular endothelial growth factor, basic fibroblastic growth factor, and microvessel density and their relation to cell proliferation in B-cell non-Hodgkin's lymphoma. Ann Diagn Pathol 2010, 14: 321–327.
22 Toomey DP, Murphy JF and Conlon KC. COX-2, VEGF and tumour angiogenesis. Surgeon 2009, 7: 174–180.
23 Hendriksen EM, Span PN, Schuuring J, Peters JP, Sweep FC, van der Kogel AJ and Bussink J. Angiogenesis, hypoxia and VEGF expression during tumour growth in a human xenograft tumour model. Microvesc Res 2009, 77: 96–103.
24 Castedo M, Perfettini JL, Roumier T and Kroemer G. Cyclin-dependent kinase-1: linking apoptosis to cell cycle and mitotic catastrophe. Cell Death Differ 2002, 9: 1287–1293.